18

Control of ROVs using a Model-free 2nd-Order Sliding Mode Approach

Tomás. Salgado-Jiménez, Luis G. García-Valdovinos and Guillermo Delgado-Ramírez
Center for Engineering and Industrial Development – CIDESI
Mexico

1. Introduction

Remotely Operated Vehicles (ROVs) have had significant contributions in the inspection, maintenance and repair of underwater structures, related to the oil industry, especially in deep waters, not easily accessible to humans. Two important capabilities for industrial ROVs are: position tracking and the dynamic positioning or station-keeping (the vehicle's ability to maintain the same position with respect to the structure, at all times).
It is important to remember that underwater environment is highly dynamic, presenting significant disturbances to the vehicle in the form of underwater currents, interaction with waves in shallow water applications, for instance. Additionally, the main difficulties associated with underwater control are the parametric uncertainties (as added mass, hydrodynamic coefficients, etc.). Sliding mode techniques effectively address these issues and are therefore viable choices for controlling underwater vehicles. On the other hand, these methods are known to be susceptible to chatter, which is a high frequency signal induced by control switches. In order to avoid this problem a High Order Sliding Mode Control (HOSMC) is proposed. The HOSMC principal characteristic is that it keeps the main advantages of the standard SMC, thus removing the chattering effects.
The proposed controller exhibits very interesting features such as: *i.* a model-free controller because it does neither require the dynamics nor any knowledge of parameters, *ii*. It is a smooth, but robust control, based on second order sliding modes, that is, a chattering-free controller is attained. *iii*. The control system attains exponential position tracking and velocity, with no acceleration measurements.
Simulation results reveal the effectiveness of the proposed controller on a nonlinear 6 degrees of freedom (DOF) ROV, wherein only 4 DOF (x, y, z, ψ) are actuated, the rest of them are considered intrinsically stable. The control system is tested under ocean currents, which abruptly change its direction. Matlab-Simulink, with Runge-Kutta ODE45 and variable step, was used for the simulations. Real parameters of the KAXAN ROV, currently under construction at CIDESI, Mexico, were taken into account for the simulations. In Figure 1 one can see a picture of KAXAN ROV.
For performance comparison purposes, numerical simulations, under the same conditions, of a conventional PID and a model-based first order sliding mode control are carried out and discussed.

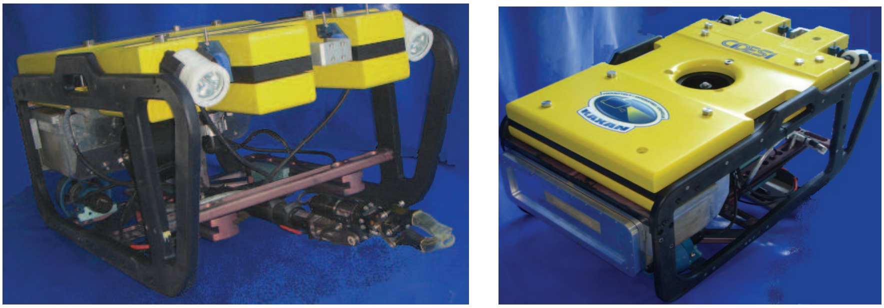

Fig. 1. ROV KAXAN; frontal view (left) and rear view (right).

1.1 Background

In this section an analysis of the state of the art is presented. This study aims at reviewing ROV control strategies ranging from position trajectory to station-keeping control, which are two of the main problems to deal with. There are a great number of studies in the international literature related to several control approaches such as PID-like control, standard sliding mode control, fuzzy control, among others. A review of the most relevant works is given below:

Visual servoing control

Some approaches use vision-based control (Van Der Zwaan & Santos-Victor, 2001)(Quigxiao et al., 2005)(Cufi et al., 2002)(Lots et al., 2001). This strategy uses landmarks or sea bed images to determine the ROV's actual position and to maintain it there or to follow a specific visual trajectory. Nevertheless, underwater environment is a blurring place and is not a practical choice to apply neither vision-based position tracking nor station-keeping control.

Intelligent control

Intelligent control techniques such as Fuzzy, Neural Networks or the combined Neuro-Fuzzy control have been proposed for underwater vehicle control, (Lee et al., 2007)(Kanakakis et al., 2004)(Liang et al., 2006). Intelligent controllers have proven to be a good control option, however, normally they require a long process parameter tuning, and they are normally used in experimental vehicles; industrial vehicles are still an opportunity area for these control techniques.

PID Control

Despite the extensive range of controllers for underwater robots, in practice most industrial underwater robots use a Proportional-Derivative (PD) or Proportional-Integral-Derivative (PID) controllers (Smallwood & Whitcomb, 2004)(Hsu et al., 2000), thanks to their simple structure and effectiveness, under specific conditions. Normally PID-like controllers have a good performance; however, they do not take into account system nonlinearities that eventually may deteriorate system's performance or even lead to instability.
The paper (Lygouras, 1999) presents a linear controller sequence (P and PI techniques) to govern x position and vehicles velocity u. Experimental results with the THETIS (UROV) are shown. The paper (Koh et al., 2006) proposes a linearizing control plus a PID technique for depth and heading station keeping. Since the linearizing technique needs the vehicle's model, the robot parameters have to be identified. Simulation and swimming pool tests show that the control is able to provide reasonable depth and heading station keeping control. An adaptive

control law for underwater vehicles is exposed in (Antonelli et al., 2008)(Antonelli et al., 2001). The control law is a PD action plus a suitable adaptive compensation action. The compensation element takes into account the hydrodynamic effects that affect the tracking performance. The control approach was tested in real time and in simulation using the ODIN vehicle and its 6 DOF mathematical model. The control shows asymptotic tracking of the motion trajectory without requiring current measurement and *a priori* exact system dynamics knowledge. Self-tuning autopilots are suggested in (Goheen & Jefferys, 1990), wherein two schemes are presented: the first one is an implicit linear quadratic on-line self-tuning controller, and the other one uses a robust control law based on a first-order approximation of the open-loop dynamics and on line recursive identification. Controller performance is evaluated by simulation.

Model-based control (Linearizing control)

Other alternative to counteract underwater control problems is the model-based approach. This control strategy considers the system nonlinearities. On the other hand it is important to notice that the system's mathematical model is needed as well as the exact knowledge of robot parameters. Calculation and programming of a full nonlinear 6 DOF dynamic model is time consuming and cumbersome. In (Smallwood & Whitcomb, 2001) a preliminary experimental evaluation of a family of model-based trajectory-tracking controllers for a full actuated underwater vehicle is reported. The first experiments were a comparison of the PD controller versus fixed model-based controllers: the Exact Linearizing Model-Based (ELMB) and the Non Linear Model-Based (NLMB) while tracking a sinusoidal trajectory. The second experiments were followed by a comparison of the adaptive controllers: adaptive exact Linearizing model-based and adaptive non linear model-based versus the fixed model-based controllers ELMB and NLMB, tracking the same trajectory. The experiments corroborate that the fixed model-based controllers outperformed the PD Controller. The NLMB controller outperforms the ELMB. The adaptive model-based controllers all provide more accurate trajectory tracking than the fixed model-based. However, notice that in order to implement such model-based controllers, at least the vehicle's dynamics is required, and in some cases the exact knowledge of the parameters as well, which is difficult to achieve in practice. In paper (Antonelli, 2006) a comparison between six controllers was performed, and four of them are model-based type; the others are a non model-based and a Jacobian-transpose-based. Numerical simulations using the 6 DOF mathematical model of ODIN were carried out. The paper concludes that the controller's effort is very similar; however the model-based approaches have a better behavior. In paper (McLain et al., 1996), real-time experiments were conducted at the Monterey Bay Aquarium Research Institute (MBARI) using the OTTER vehicle. The control strategy was a model-based linearizing control. Additionally interaction forces acting on the vehicle due to arm motion were predicted and fed into the vehicle's controller. Using this method, station-keeping capability was greatly enhanced. Finally, other exact linearizing model-based control has been used in (Ziani-Cherif, 19998).

First order Sliding Mode Control (SMC)

Sliding mode techniques effectively address underwater control issues and are therefore viable choices for controlling underwater vehicles. However, it is well known that these methods are susceptible to chatter, which is a high frequency signal induced by the switching control. Some relevant studies that use SMC are described next. The paper (Healey & Lienard, 1993) used a sliding mode control for the combined steering, diving and speed control. A series of simulations in the NPS-AUV 6 DOF mathematical model are conducted. (Riedel, 2000) proposes a new Disturbance Compensation Controller (DCC), employing on board vehicles sensors that allow the robot to learn and estimate the seaway dynamics. The estimator is based on a Kalman filter and the control law is a first order sliding mode, which induces harmful high frequency signals on the actuators. The paper (Gomes et al., 2003) shows some control techniques tested in PHANTON 500S simulator. The control laws are: conventional PID, state feedback linearization and first order sliding modes control. The author presented a comparative analysis wherein the sliding mode has the best performance, at the expense of a high switching on the actuators. Work (Hsu et al., 2000) proposes a dynamic positioning system for a ROV based on a mechanical passive arm, as a measurement system. This measurement system was selected from a group of candidate systems, including long base line, short baseline, and inertial system, among others. The selection was based on several criteria: precision, construction cost and operational facilities. The position control laws were a conventional P-PI linear control. Last, the other position control law was the variable structure model-reference adaptive control (VS-MRAC). Finally, in the paper (Sebastián, 2006) a model-based adaptive fuzzy sliding mode controller is reported.

Adaptive first order Sliding Mode Control (ASMC)

SMC have a good performance when the controller is well tuned, however if the robot changes its mass or its center of mass, for instance, because of the addition of a new arm or a tool, the system dynamics changes and the control performance may be affected; similarly, if a change in the underwater disturbances occurs (current direction, for instance), a new tuning should be done. In order to reduce chattering problems, ASMC have been proposed. These controllers are excellent alternative to counteract changes in the system dynamics and environment, nevertheless design and tuning time could be longer, and robot model is required. Following, some relevant works are enumerated. In (Da Cunha, 1995), an adaptive control scheme for dynamic positioning of ROVs, based on a variable structure control (first order sliding mode), is proposed. This sliding mode technique is compared with a P-PI controller. Their performances are evaluated by simulation and in pool tests, proving that the sliding mode approach has a better result. The paper (Bessa, 2007) describes a depth SMC for remotely operated vehicles. The SMC is enhanced by an adaptive fuzzy algorithm for uncertainties/disturbances compensation. Numerical simulations in 1 DOF (depth) are presented to show the control performance. This SMC also uses the vehicle estimated model.
Paper (Sebastián & Sotelo, 2007) proposes the fusion of a sliding mode controller and an adaptive fuzzy system. The main advantage of this methodology is that it relaxes the required exact knowledge of the vehicle model, due to parameter uncertainties are compensated by the fuzzy part. A comparative study between; PI controller, classic sliding mode controller and the adaptive fuzzy sliding mode is carried out. Experimental results demonstrate the good performance of the proposed controller. (Song & Smith, 2006) combine sliding mode control with fuzzy logic control. The combination objective is to reduce chattering effect due to model parameter uncertainties and unknown perturbations. Two control approaches are tested: Fuzzy Sliding Mode Controller (FSMC) and Sliding Mode Fuzzy Controller (SMFC). In the FSMC uses a simple fuzzy logic control to fuzzify the relationship of the control command and the distance between the actual state and the sliding surface. On the other hand, at the SMFC each rule is a sliding mode controller. The boundary layer and the coefficients of the sliding surface become the coefficients of the rule output function. Open water experiments were conducted to test AUV's depth and heading controls. The better behavior was detected in the

SMFC. Finally, an adaptive first order sliding mode control for an AUV for the diving maneuver was implemented in (Cristi et al., 1990). This control technique combines the adaptivity of a direct adaptive control algorithm with the robustness of a sliding mode controller. The control is validated by numerical simulations.

High Order Sliding Mode Control (HOSMC)

In order to avoid chattering problem and system model requirement a new methodology called High Order Sliding Mode Control (HOSMC) is proposed in (Garcia-Valdovinos, 2009). HOSMC principal characteristic is that it keeps the main advantages of the standard SMC, removing the chattering effects (Perruquett & Barbot, 1999).
The methodology proposed in this chapter was firstly reported in (Garcia-Valdovinos, 2009), where it is proposed a second order sliding-PD control to address the station keeping problem and trajectory tracking under disturbances. The control law is tested in an under-actuated 6-DOF ROV under Matlab-Simulink simulations, considering unknown and abrupt changing currents direction.

2. General 6 DOF underwater system model

Following standard practice (Fossen, 2002), a 6 DOF nonlinear model of an underwater vehicle is obtained. By using a global reference *Earth-fixed frame* and *Body-fixed frame*, see Figure 2. The *Body-fixed frame* is attached to the vehicle. Its origin is normally on the center of gravity. The motion of the *Body-fixed frame* is described relative to the *Earth-fixed frame*.

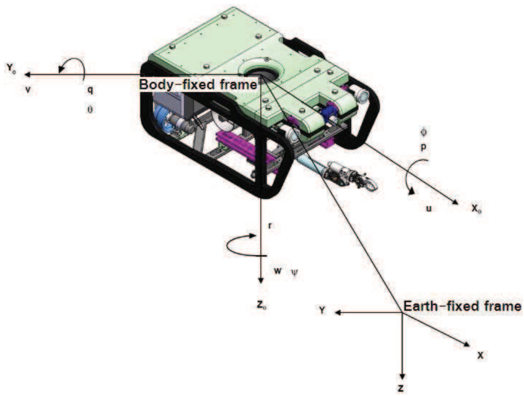

Fig. 2. Reference Earth-fixed frame and Body-fixed frame.

The notation defined by SNAME (Society of Naval Architects and Marine Engineers) established that the *Body-fixed frame* has components of motion given by the linear velocities vector $\nu_1 = \begin{bmatrix} u & v & w \end{bmatrix}^T$ and angular velocities vector $v_2 = \begin{bmatrix} p & q & r \end{bmatrix}^T$ (Fossen, 2002).. The general velocity vector is represented as:

$$\nu = \begin{bmatrix} \nu_1 & \nu_2 \end{bmatrix}^T = \begin{bmatrix} u & v & w & p & q & r \end{bmatrix}^T$$

where u is the linear velocity in surge, v the linear velocity in sway, w the linear velocity in heave, p the angular velocity in roll, q the angular velocity in pitch and r the angular velocity in yaw.

The position vector $\eta_1 = \begin{bmatrix} x & y & z \end{bmatrix}^T$ and orientation vector $\eta_2 = \begin{bmatrix} \phi & \theta & \psi \end{bmatrix}^T$ coordinates expressed in the Earth-fixed frame are:

$$\eta = \begin{bmatrix} \eta_1 & \eta_2 \end{bmatrix}^T = \begin{bmatrix} x & y & z & \phi & \theta & \psi \end{bmatrix}^T$$

where *x, y, z* represent the Cartesian position in the *Earth-fixed frame* and φ represent the roll angle, θ the pitch angle and ψ the yaw angle.

Kinematic model. It is the transformation matrix between the Body and Earth frames, expressed as (Fossen, 2002):

$$\dot{\eta} = J(\eta)\nu$$
$$\begin{bmatrix} \dot{\eta}_1 \\ \dot{\eta}_2 \end{bmatrix} = \begin{bmatrix} J_1(\eta_2) & 0_{3x3} \\ 0_{3x3} & J_2(\eta_2) \end{bmatrix} \begin{bmatrix} \nu_1 \\ \nu_2 \end{bmatrix} \tag{1}$$

where $J_1(\eta_2)$ is the rotation matrix that gives the components of the linear velocities ν_1 in the *Earth-fixed frame* and $J_2(\eta_2)$ is the matrix that relates angular velocity ν_2 with vehicle's attitude in the global reference frame.

Well-posed Jacobian: The transformation (1) is ill-posed when $\theta = \pm 90^o$. To overcome this singularity, a quaternion approach might be considered. However, the vehicle KAXAN is not required to be operated on $\theta = \pm 90^o$. In addition, the ROV is completely stable in roll and pitch coordinates.

Hydrodynamic model: The equation of motion expressed in the *Body-fixed frame* is given as follows (Fossen, 2002):

$$M\dot{\nu} + C(\nu)\nu + D(\nu)\nu + g(\eta) = \tau \tag{2}$$

where $\nu \in R^{n6\,x\,1}$, $\eta \in R^{nx1}$, and $\tau \in R^{p\,x\,1}$. τ denotes the control input vector. Matrix $M \in R^{nxn}$, is the inertia matrix including hydrodynamic added mass, $C \in R^{n\,x\,n}$, is a nonlinear matrix including Coriolis, centrifugal and added terms, $D \in R^{n\,x\,n}$, denotes dissipative influences, such as potential damping, viscous damping and skin friction, finally vector $g \in R^{n\,x\,1}$, denotes restoring forces and moments.

Ocean currents. Some factors that generate current are: tide, local wind, nonlinear waves, ocean circulation, density difference, etc. It's not the objective of this work to make a deeply study of this phenomena, but only to study the current model proposed by (Fossen, 2002). This methodology proposes that the equations of motion can be represented in terms of the relative velocity:

$$\nu_r = \nu - V_c \tag{3}$$

where $V_c = \begin{bmatrix} u_c & v_c & w_c & 0 & 0 & 0 \end{bmatrix}^T$ is a vector of irrotation Body-fixed current velocities.

The average current velocity V_c is related to Earth-fixed current velocity components $\begin{bmatrix} u_c^E & v_c^E & w_c^E \end{bmatrix}$ by the following expression:

$$\begin{aligned} u_c^E &= V_c \cos(\alpha_c)\cos(\beta_c) \\ v_c^E &= V_c \cos(\beta_c) \\ w_c^E &= V_c \sin(\alpha_c)\cos(\beta_c) \end{aligned} \tag{4}$$

where α_c is the angle of attack and β_c the sideslip angle.
Finally, the Earth-fixed current velocity could be computed at the Body-fixed frame, by using

$$\begin{bmatrix} u_c \\ v_c \\ w_c \end{bmatrix} = J_1(\eta_2) \begin{bmatrix} u_c^E \\ v_c^E \\ w_c^E \end{bmatrix} \tag{5}$$

In order to simulate the current and their effect on the ROV, the following model will be applied

$$M\dot{\nu} + C_{RB}(\nu)\nu + C_A(\nu_r)\nu_r + D(\nu_r)\nu_r + g(\eta) = \tau \tag{6}$$

where C_{RB} is the Coriolis from rigid body inertia, and C_A is the Coriolis from added mass.
Assuming that Body-fixed current velocity is constant or at least slowly varying, $\dot{v}_c = 0 \quad \Rightarrow \quad \dot{v}_r = \dot{v}$.

Control input vector. The τ_η comprises the thruster force applied to the vehicle. KAXAN has four thrusters, whose forces and moments are distributed as:

- F_1 Thruster located at rear (left).
- F_2 Thruster located at rear (right).
- F_3 Lateral thruster.
- F_4 Vertical thruster.

F_1 and F_2 propel the vehicle in the x direction and generates the turn in ψ when $F_1 \neq F_2$, F_3 propels the vehicle sideways (y direction) and F_4 allows the vehicle to move up and down (z direction). Then the control signal τ_η must be multiplied by a $\boldsymbol{B}$ matrix comprising forces and moments according to the force application point to the center of mass.

$$\tau_\eta = \begin{bmatrix} F_1 + F_2 \\ F_3 \\ F_4 \\ -F_3 d_{3z} + F_4 d_{4y} \\ F_1 d_{1z} + F_2 d_{2z} - F_4 d_{4x} \\ -F_1 d_{1y} + F_2 d_{2y} - F_3 d_{3x} \end{bmatrix} \tag{7}$$

Rewriting (7) gives rise to

$$\tau_\eta = \underbrace{\begin{bmatrix} X \\ Y \\ Z \\ K \\ M \\ N \end{bmatrix}}_{Control\ \ Force} = \underbrace{\begin{bmatrix} 1 & 1 & 0 & 0 \\ 0 & 0 & 1 & 0 \\ 0 & 0 & 0 & 1 \\ 0 & 0 & -d_{3z} & d_{4y} \\ d_{1z} & d_{2z} & 0 & -d_{4x} \\ -d_{1y} & d_{2y} & d_{3x} & 0 \end{bmatrix}}_{B} \begin{bmatrix} F_1 \\ F_2 \\ F_3 \\ F_4 \end{bmatrix} \tag{8}$$

3. Control systems

In this section the PID control and model-based first order SMC laws are reminded, later the model-free 2-order sliding mode control technique is introduced (hereafter called HOSMC). These control laws behavior are shown in the next section.

3.1 PID control

The Proportional-Integral-Derivative control law is (Ogata, 1995):

$$\begin{aligned} \tau \;=\; & K_P e(k\Delta_T) + \frac{K_P \Delta_T}{T_I} \sum_{h=1}^{k} \frac{e(h\Delta_T) + e((h-1)\Delta_T)}{2} \\ & + K_P T_D \left[e(k\Delta_T) - e((k-1)\Delta_T) \right] \end{aligned} \tag{9}$$

where Δ_T is the sample time, $e(k\Delta_T)$ is the error measured at the sample time $k\Delta_T$. K_P is the proportional gain, T_I is the integral time and T_D is the derivative time. The PID control gains are shown in Table 1.

	Gains					
	x	y	z	ϕ	θ	ψ
K_p	1600	1800	1300	0	0	18000
T_d	3000	15000	3000	0	0	70000
T_i	0.5	10	0.5	0	0	0.25

Table 1. PID control gains.

3.2 Model-based first order sliding mode control (SMC)

Using the methodology given in (Slotine & Li, 1991), the sliding surface is defined as

$$s = \dot{\tilde{\eta}} - \alpha \tilde{\eta} \tag{10}$$

where $\tilde{\eta} = \eta - \eta_d$.

The SMC control law is given by

$$\tau = \tau_{eq} + K_s sign(\beta s) \tag{11}$$

where τ_{eq} is the equivalent control given by the system estimated dynamic. Parameters β and K_s are constants, *sign* denotes the sign function. Table 2 lists the control gains used in the simulation.

	Gains					
	x	y	Z	ϕ	θ	ψ
K_s	530	700	10	0	0	40
α	530	500	25	0	0	15

Table 2. SMC control gains.

3.3 Model-free 2nd-order sliding mode control (HOSMC)

To analyze the proposed controller is necessary to introduce the following preliminaries. Let the nominal reference $\dot{\eta}_r$ be:

$$\dot{\eta}_r = \dot{\eta}_d - \alpha\tilde{\eta} + S_d - K_i \int_0^t sign\left(S_q\right) d\sigma \tag{12}$$

where α, K_i are diagonal positive definite $n \times n$ gain matrices, function $sign(x)$ stands for sign function of $x \in \Re^n$, and

$$\begin{aligned} S_q &= S - S_d \\ S &= \dot{\tilde{\eta}} - \alpha\tilde{\eta} \\ S_d &= S(t_0)\ e^{-\kappa\ t} \end{aligned} \tag{13}$$

for $\kappa > 0$. $S(t_0)$ stands for $S(t)$ at $t=0$.
Now, let the extended error variable be defined as follows:

$$S_r = \dot{\eta} - \dot{\eta}_r \tag{14}$$

and substituting (12) into (14) yields,

$$S_r = S_q + K_i \int_0^t sign\left(S_q\right) d\sigma \tag{15}$$

Notice that the task is defined in the *Earth-fixed frame* for the sake of simplicity.

Controller definition

The control design and some structural properties are now given.
Theorem. Consider the vehicle dynamics (2) in closed loop with the control law given by

$$\tau_\eta = -K_d S_r \tag{16}$$

where K_d is a positive $n \times n$ feedback gain matrix. Exponential tracking is guaranteed, provided that K_i in (15) and K_d are large enough, for small initial error condition.
Proof. A detailed analysis shows that the above Theorem fulfills, see (Garcia-Valdovinos et al. 2006) and (Parra-Vega et al., 2003) for more details ■.
Remark 1. Since the control (15) is computed in the Earth-fixed frame it is necessary to map it into the Body- fixed frame by using the transpose Jacobian (1) as follows:

$$\tau = J^T \tau_\eta \tag{17}$$

Remark 2. Expanding the control law (16) can be rewritten as follows:

$$\tau_\eta = -\underbrace{K_d\alpha\tilde{\eta}}_{P} - \underbrace{K_d\dot{\tilde{\eta}}}_{D} - \underbrace{K_d K_i \int_0^t sign\left(S_q\right) d\sigma}_{Sliding\ part} \tag{18}$$

which gives rise to a sliding PD-like controller.

3.3.1 Comments on HOSMC

How to tune the controller: The stability proof (see (Garcia-Valdovinos et al. 2006) and (Parra-Vega et al., 2003) for more details) suggests that arbitrary small K_i and small α can be set as a starting point. Increase feedback gain K_d until acceptable boundedness of S_r appears.

Then, increase gradually K_i until the sliding mode arises. Finally, increase α to achieve a better position tracking performance. Notice that K_i is not a high gain result since a larger K_i does not mean a larger domain of stability.

Robustness: The system has inherent robustness of typical variable structure systems, since the invariance property is attained for all time, whose convergence is governed solely by (13) when $S_q(t)=0$ for all time, independently of bounded disturbances.

Smooth Controller: Higher-order sliding modes, in this case second order sliding mode (SOSM), have emerged to solve the problem of chattering, which is induced by first order sliding modes (FOSM). Besides preserving the advantages of FOSM, the scheme SOSM totally removes the chattering effect of FOSM, and provides for even higher accuracy. In our case, SOSM is induced, and chattering is circumvented by integrating the sign function of S_q.

Finite time convergence: Since sliding mode exists for all time, it is possible to attain finite time convergence of position tracking errors by means of well-posed terminal attractors. Finite time convergence can be tuned arbitrarily via a time-varying gain $\alpha(t)$ so as to drive smoothly $\Delta x(t)$ toward its equilibrium $\Delta x(t)=0$. Gain $\alpha(t)$ is tailored with a Time Base Generator (TBG), which may be a fifth order polynomial that smoothly goes from $0 \rightarrow 1$, for more details see (Garcia-Valdovinos et al. 2006).

4. Numerical simulations

Performance of the controllers is verified through some simulations with a 6 DOF underwater vehicle (2), where only 4 DOF are actuated, that is (x, y, z, ψ). Evidently, ϕ and θ are not actuated, though these are bounded (stable). Position tracking simulations are presented. Matlab-Simulink has been used to perform the simulations with ODE Runge-Kutta 45, variable step.

4.1 Controller's gains

Feedback gains for the controller are show in Table 3.

	Gains					
	x	y	z	ϕ	θ	ψ
α	30	30	30	0	0	50
K_d	1000	1000	1000	0	0	1000
K_i	0.05	0.05	0.05	0	0	0.05
κ	5					

Table 3. Model-free 2-order sliding mode contol gains.

4.2 Ocean current parameters

The current starts flowing to the north and after some time, it suddenly changes to east. In all cases the current is V_c=1.1 *m/s*. According to (2) and (4) one has the following:

1. North: When flowing to the north, parameters are the following: $\alpha_c = 0$ *rad* and $\beta_c = 0$ *rad*.
2. East: When flow is in the east direction, parameters are the following: $\alpha_c = 0$ *rad* and $\beta_c = \pi/2$ *rad*.

4.3 Position tracking

Now, the proposed controller is evaluated for tracking tasks, under ocean currents. The task is divided into two stages. First stage consists of moving the vehicle smoothly from an initial position $[x_i, y_i, z_i, \psi_i]$ = [0, 0, 0, 0] to a final position $[x_f, y_f, z_f, \psi_i]$=[1, 0, 0.5, π/2], see the linear path in figures 3, 7 and 11, for the PID, SMC and HOSMC, respectively. This stage lasts 15 seconds, from $t=0\ s$ to $t=15\ s$.

Second stage, once the vehicle is correctly oriented, it is requested to follow a circumference of radio $r=1\ m$, centered at (h, k) = (0, 0). The circumference is executed at a rate given by $\omega=0.628\ rad/s$, that is, in $t=10\ s$. Notice that the circumference is designed in plane x, y, and ψ is always tangential to the circumference, see the circular path in figures (3, 7 and 11, for the PID, SMC and 2-order sliding mode control, respectively). This stage lasts 10 seconds, from $t>15\ s$ to $t=25\ s$.

From $t=10\ s$ to $t<15\ s$ (first stage) the ocean current flows to the north (u_c). The lasts 15 seconds, from $t>10\ s$ to $t=25\ s$, current flows to the east (υ_c).

4.4 Description of results

Figures 3 (PID), 7 (SMC) and 11 (HOSMC), depict the complete trajectory tracking by the system.

Figures 4 (PID), 8 (SMC) and 12 (HOSMC), show the system position tracking comparison x vs x_d, y vs y_d and z vs z_d.

Figures 5 (PID), 9 (SMC) and 13 (HOSMC), give the robot inclination behavior; notice that the angular position tracking in ψ is attained (even under currents influence). As it was mentioned ϕ and θ are not actuated, however they are stable, they present a slight deviation from zero, due to the changing current.

The control signal behavior is described in Figures 6 for the PID control, 10 for the SMC and 14 for the HOSMC. The figures show the propulsion force in the x, y and z directions (from top to bottom), and the last box represent the momentum around in the ψ angle.

Finally the control performance is compared by using the Mean Square Error (MSE). Figure 15 represents the MSEs values for the three control techniques. The figure show two bars for each control technique, the first represents the MSE_R and the second is the MSE_ψ. Where the MSE_R is defined by:

$$MSE_R = \sqrt{(MSE_x)^2 + (MSE_y)^2 + (MSE_z)^2} \tag{19}$$

4.5 PID control

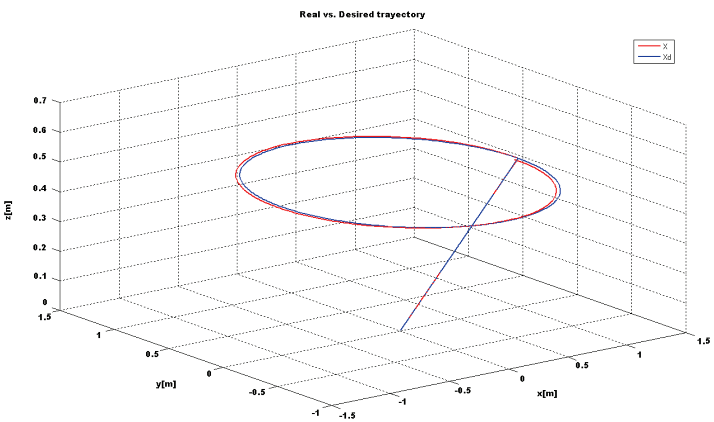

Fig. 3. Position tracking performance under PID control.

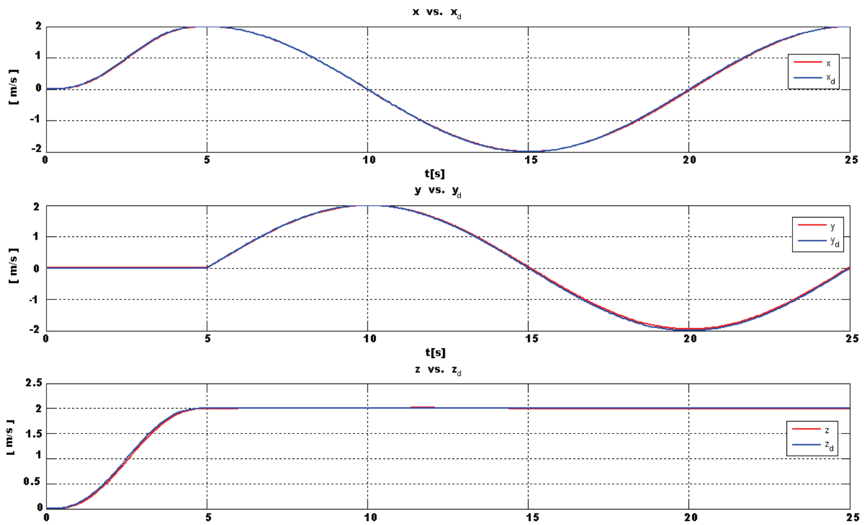

Fig. 4. Position tracking performance (x *vs* x_d, y *vs* y_d and z *vs* z_d) under the PID control.

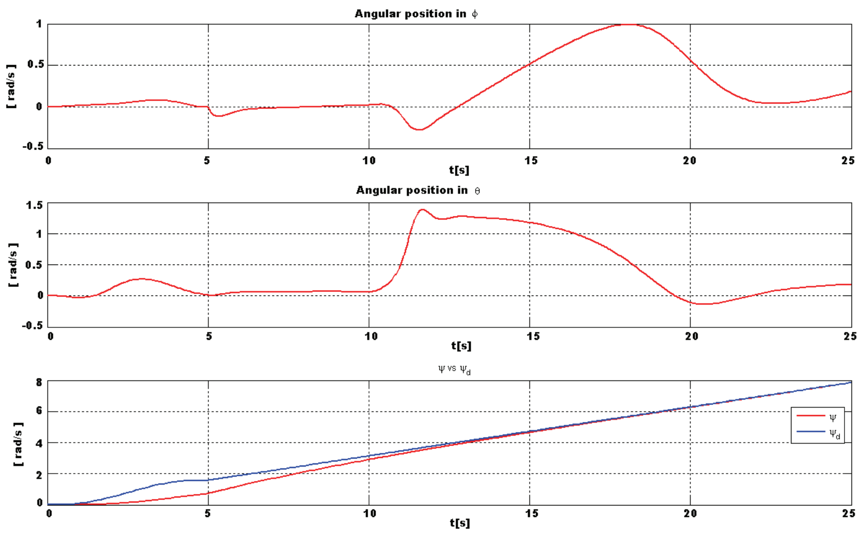

Fig. 5. Angular inclinations behavior (ϕ, θ and ψ *vs* ψ_d) under the PID control.

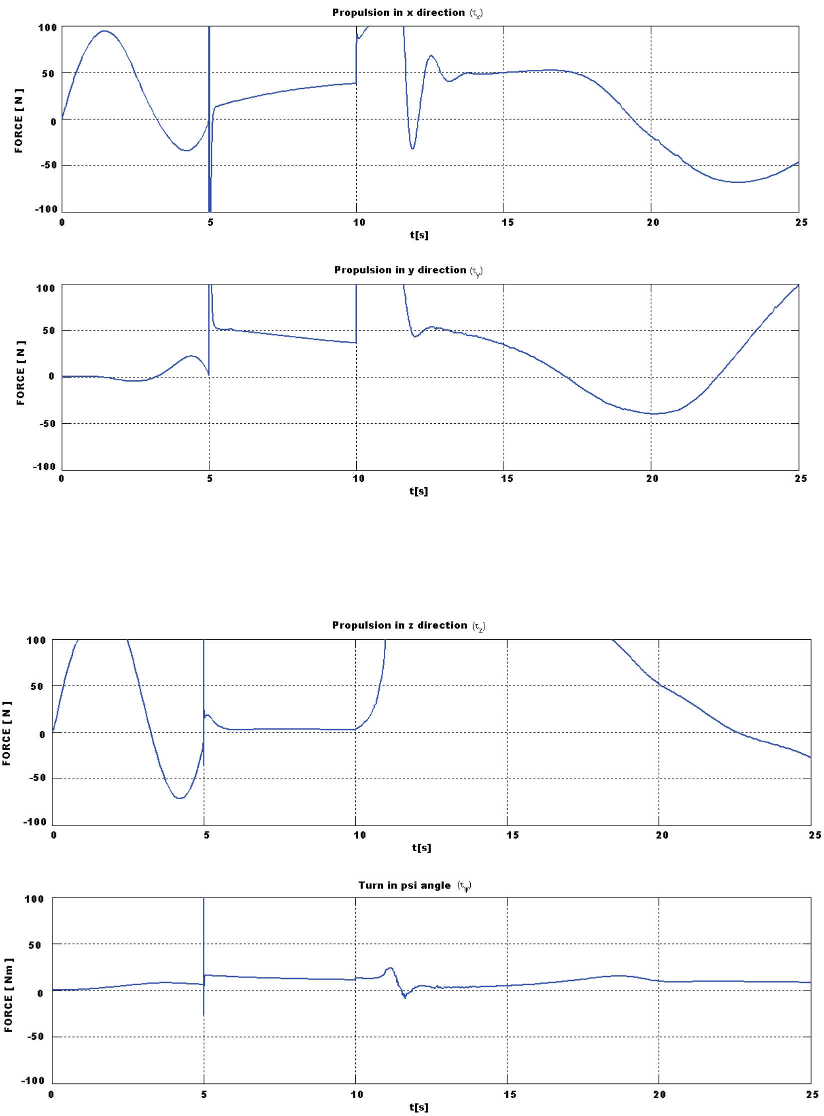

Fig. 6. Control signal behavior. From top to bottom propulsion force in the x, y and z directions, and the last box represent the momentum around the ψ angle (PID control).

4.6 Model-based first order mode control (SMC)

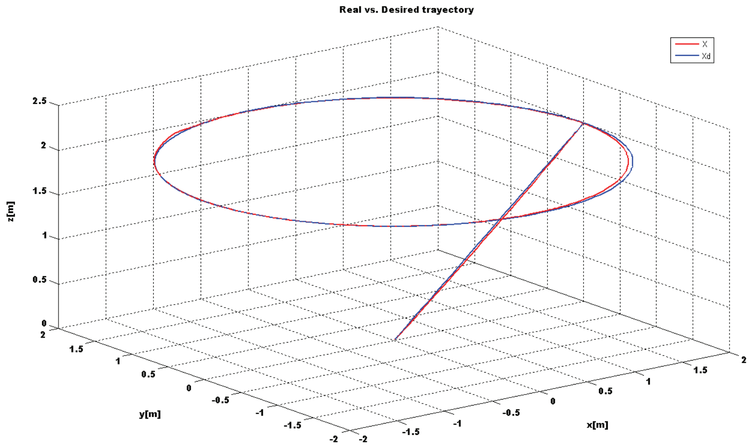

Fig. 7. Position tracking performance with SMC.

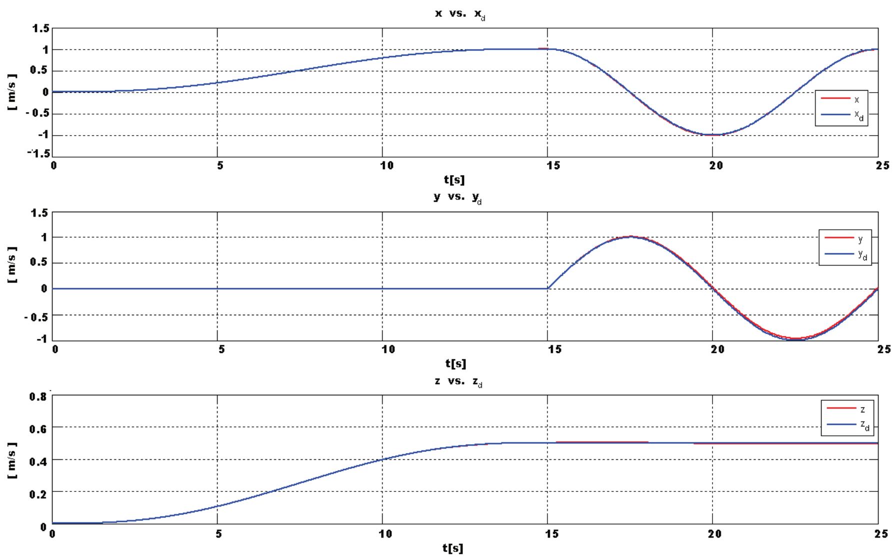

Fig. 8. Position tracking performance (x *vs* x_d, y *vs* y_d and z *vs* z_d) with the SMC.

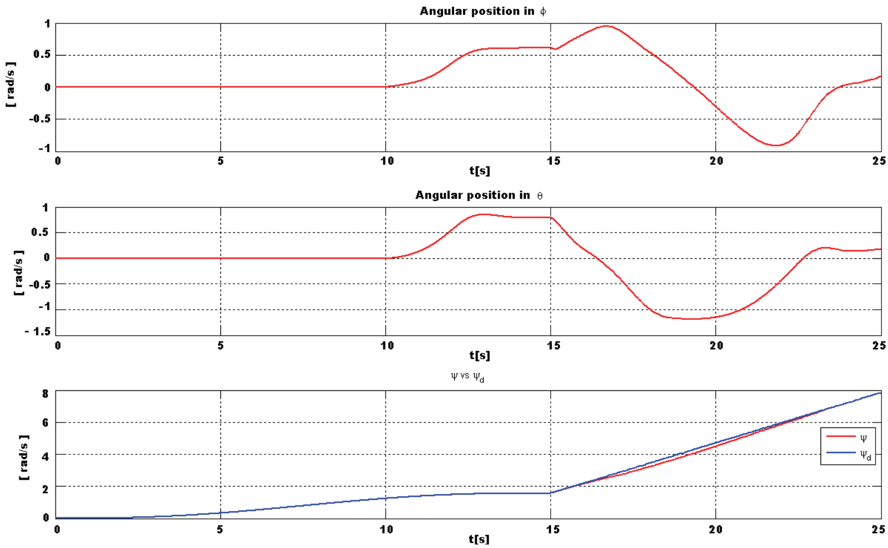

Fig. 9 Angular inclinations behavior (ϕ, θ and ψ *vs* ψ_d) with the SMC control.

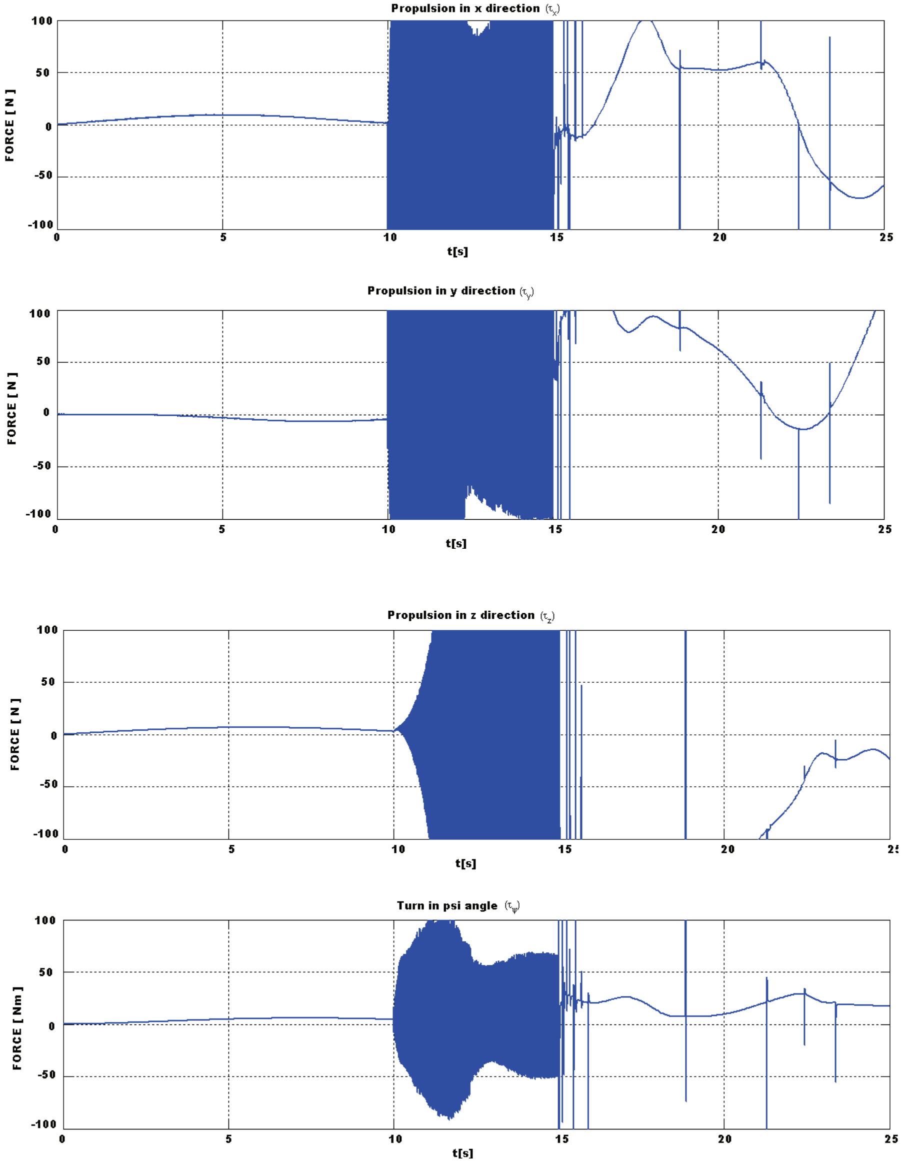

Fig. 10. Control signal behavior. From top to bottom propulsion force in the x, y and z directions, and the last box represent the momentum around in the ψ angle (SMC).

4.7 Model-free 2nd-Order sliding mode control

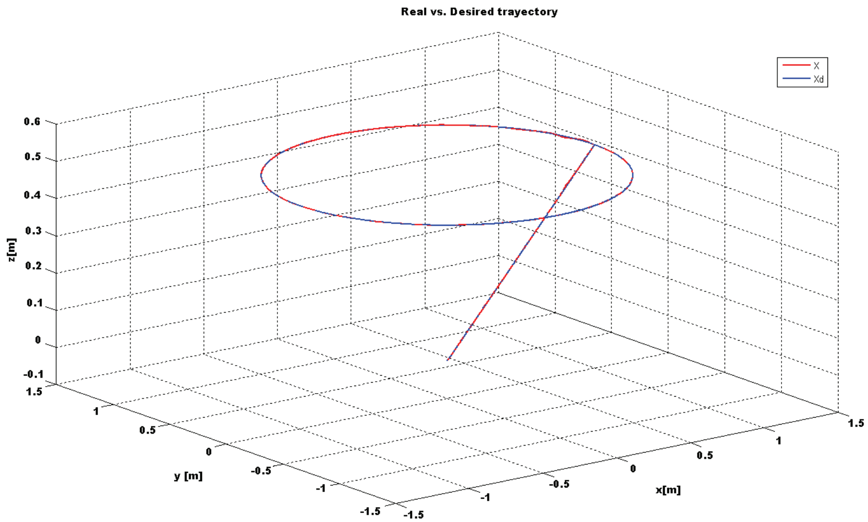

Fig. 11. Position tracking performance with HOSMC.

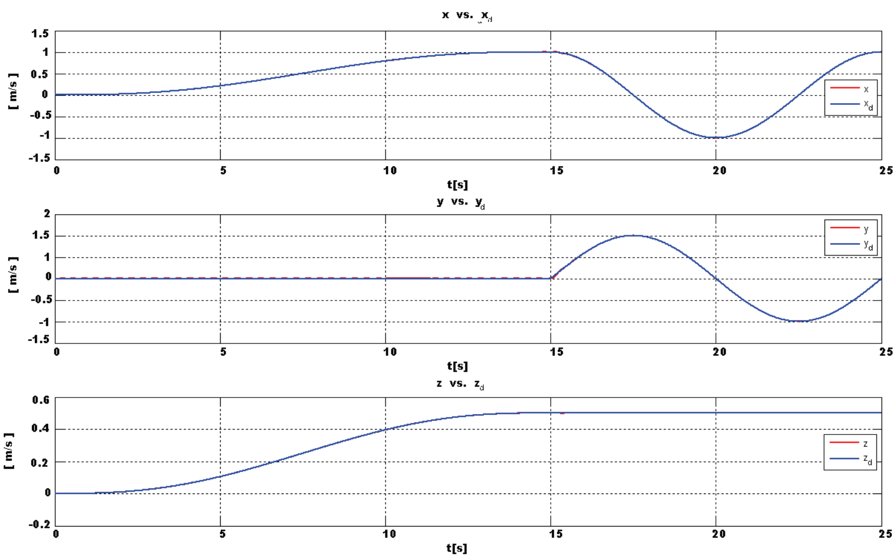

Fig. 12. Position tracking performance (x *vs* x_d, y *vs* y_d and z *vs* z_d) with the HOSMC.

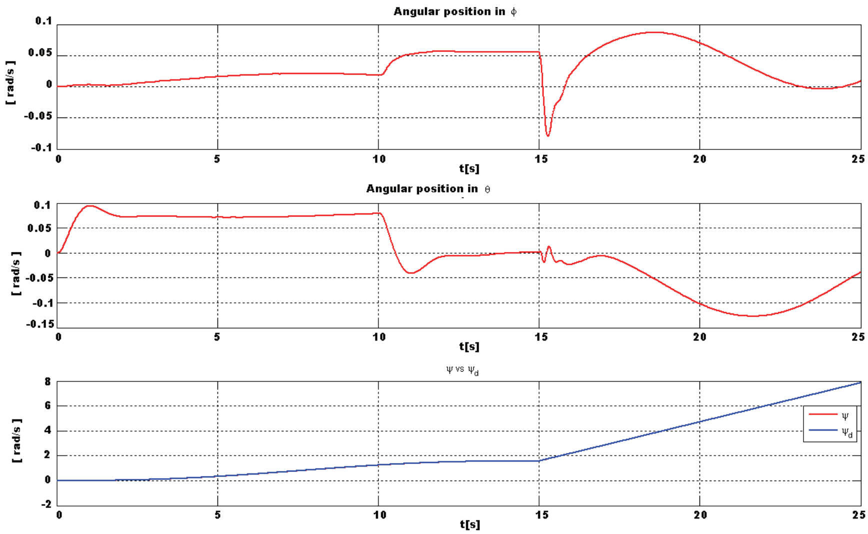

Fig. 13. Angular inclinations behavior (ϕ, θ and ψ *vs* ψ_d) with the HOSMC.

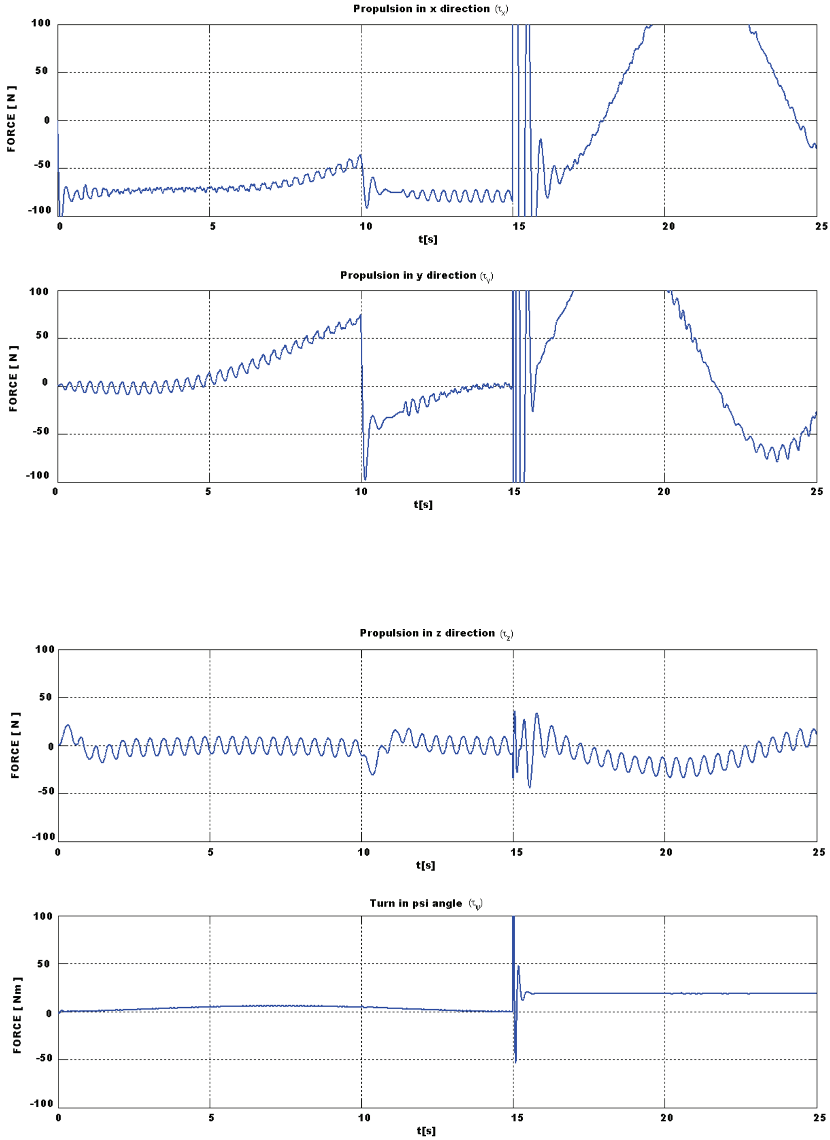

Fig. 14. Control signal behavior. From top to bottom propulsion force in the x, y and z directions, and the last box represent the momentum around in the ψ angle (HOSMC).

4.8 Control performance comparison by Mean Square Error (MSE)

An MSE study reveals that the proposed controller (HOSMC) exhibits the best performance in terms of position tracking.

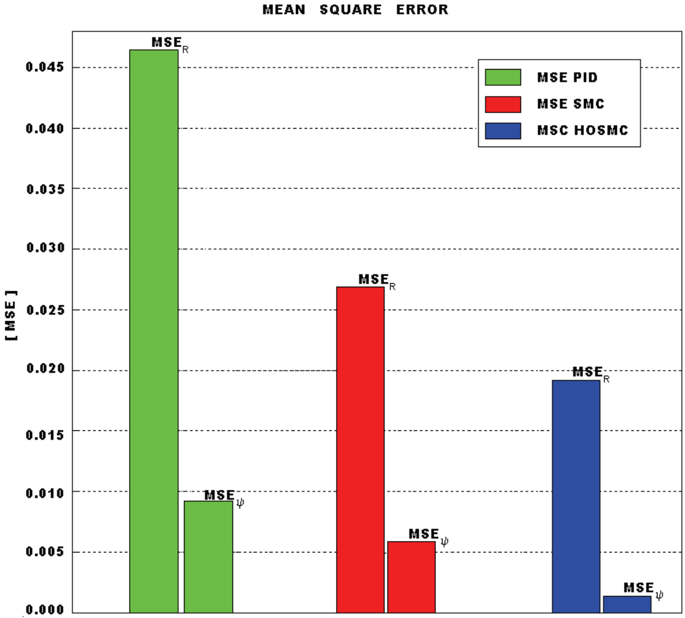

Fig. 15. Mean Square Error (MSE) values for the three control techniques.

5. References

Antonelli, G. (2006). Dynamic Control of 6-DOF AUVs. *Springer Tracts in Advanced Robotics*, Volume 2.

Antonelli, G.; Chiaverini, S.; Sarkar, N. & West, M. (2001). Adaptive control of an autonomous underwater vehicle: experimental results on ODIN. *Transactions on Control Systems Technology, IEEE, Sep 2001.*

Antonelli, G.; Fossen, T. I. & Yoerger, D. R. (2008). Underwater Robotics, *Springer Handbook of Robotics, Springer Berlin Heidelberg*.

Bessa, W. M.; Dutra, M. S. & Kreuzer, E. (2007). Depth control of remotely operated underwater vehicles using an adaptive fuzzy sliding mode controller. *Robotics and Autonomous system, Elsevier.*

Cristi, R.; Papoulias, F. A. & Healey, A. J. (1990). Adaptive sliding mode control of autonomous underwater vehicles in the dive plane. *IEEE Journal of Oceanic Engineering*, Vol. 15, No. 15 July 1990.

Cufi, X.; Garcia, R. & Ridao. P. (2002). An approach to vision-based station keeping for an unmanned underwater vehicle. IEEE/RSJ International Conference on Intelligent Robots and System.

Da Cunha, J.P.V.S.; Costa, R.R. & Liu, Hsu. (1995). Design of a high performance veriable structure position control of ROV's. *IEEE Journal of Oceanic Engineering*, Volume 20, No. 1, Page(s):42 – 54, Jan.

Fossen, T. I. (2002). *Marine control systems; guidance, navigation and control of ships. Rigs and underwater vehicles.* Marine Cybernetics.

García-Valdovinos, L. G.; Parra-Vega, V. & Arteaga, M.A. (2006). Bilateral Cartesian Sliding PID Force/Position Control for Tracking in Finite Time of Master-Slave Systems, *Proceedings of the IEEE ACC'06*, pp. 369-375, Minneapolis, Minnesota, EUA.

Garcia-Valdovinos, L. G.; Salgado-Jimenez. T. & Torres-Rodríguez, H. (2009). Model-free high order sliding mode control for ROV: Station-keeping approach, *Proceedings of OCEANS MTS/IEEE.*

Goheen K. R. & Jefferys E.R. (1990). Multivariable self-tuning autopilots for autonomous and remotely operated underwater vehicles. *IEEE Journal of Oceanic Engineering.* Jul.

Gomes, R. M. F.; Sousa, J. B. & Pereira, F. L. (2003). Modelling and control of the IES project ROV. *Proceedings of European control conference*, Cambridge, UK.

Healey, A. J. & Lienard, D. (1993). Multivariable sliding mode control for autonomous diving and steering of unmanned underwater vehicles. *IEEE Journal of Oceanic Engineering,* Vol. 18, No. 3, July.

Hsu L.; Costa, R. R. & Lizarralde, F. (2000). Dynamic positioning of remotely operated underwater vehicles. *IEEE Robotics and Automation Magazine*. September, 2000.

Kanakakis, V.; Valavanis, K. P. & Tsourveloudis, N. C. (2004). Fuzzy-Logic Based Navigation of Underwater Vehicles. *Journal of Intelligent and Robotic Systems*, Springer Netherlands, Volume 40, Number 1 / May.

Koh, T. H.; Lau, M. W. S.; Seet, G. & Low, E., A. (2006). Control Module Scheme for an Underactuated Underwater Robotic Vehicle. *Journal of Intelligent and Robotic Systems,* Springer Netherlands. Volume 46, Number 1,/ May.

Lee, J.; Roh, M.; Lee, J. & Lee, D. (2007). Clonal Selection Algorithms for 6-DOF PID Control of Autonomous Underwater Vehicles. *Lecture Notes in Computer Science*, Springer Berlin / Heidelberg. Volume 4628/2007.

Liang, X.; Li, Y.; Xu, Y.; Wan, L. & Qin, Z. (2006). Fuzzy neural network control of underwater vehicles based on desired state programming. *Journal of Marine Science and Application*, Harbin Engineering University. Volume 5, Number 3 / September.

Lots, J.-F.; Lane, D.M.; Trucco, E. & Chaumette, F. (2001). A 2D visual servoing for underwater vehicle station keeping. *Proceedings of the IEEE International Conference on Robotics and Automation,* ICRA2001.

Lygouras, J. N. (1999). DC Thruster Controller Implementation with Integral Anti-wind up Compensator for Underwater ROV. *Journal of Intelligent and Robotic Systems,* Springer Netherlands. Volume 25, Number 1 / May.

McLain, T. W.; Rock, S. M. & Lee, M. J. (1996). Experiments in the coordinated control of an underwater arm/vehicle system. *Autonomous Robots,* Springer Netherlands. Vol. 3, Numbers 2-3 / June.

Ogata, K. (1995). *Discrete-Time Control Systems.* 2nd Edition, Prentice-Hall.

Parra-Vega, V.; Arimoto, S.; Liu, Y. H.; Hirzinger, G. & Akella, P. (2003). Dynamic sliding PID control for tracking of robot manipulators: Theory and experiments. *IEEE Trans. on Rob. and Autom.*, 19(6):967--976, December.

Perruquett, W. & Barbot, J. P. (1999). *Sliding Modes control in Engineering*. Marcel Dekker, Inc.

Qingxiao, W.; Shuo, L., Yingming, H. & Feng, Z. (2005). A model-based monocular vision system for station keeping of an underwater vehicle. *Proceedings of the IEEE International Conference on Robotics and Biomimetics (ROBIO)*.

Sebastián, E. (2006). Adaptive Fuzzy Sliding Mode Controller for the Snorkel Underwater Vehicle. *Lecture Notes in Computer Science*, Springer Berlin / Heidelberg, Volume 4095/2006.

Sebastián, E. & Sotelo, M. A. (2007). Adaptive Fuzzy Sliding Mode Controller for the Kinematic Variables of an Underwater Vehicle. *Journal of Intelligent and Robotic Systems,* Springer Netherlands, Volume 49, Number 2, June.

Slotine J.-J. and W. Li. (1991). *Applied Nonlinear Control.* Prentice-Hall.

Smallwood, D. A. & Whitcomb, L. L. (2001). Toward Model Based dynamic Positioning of underwater robotics Vehicles. *Proceedings of the OCEANS MTS/IEEE.*

Smallwood, D.A. & Whitcomb, L. L. (2004). Model-based dynamic positioning of underwater robotic vehicles: theory and experiment. *IEEE Journal of Oceanic Engineering,* Volume 29, Issue 1, Page(s):169 – 186, January.

Song, F. & Smith, S. M. (2006). Combine Sliding Mode Control and Fuzzy Logic Control for Autonomous Underwater Vehicles. *Lecture Notes in Advanced Fuzzy Logic Technologies in Industrial Applications,* Publisher Springer London.

Riedel, J. S. (2000). Shallow water station-keeping of an autonomous underwater vehicle: The experimental Results of a disturbance compensation controller. *Proceedings of the OCEANS MTS/IEEE.*

Van Der Zwaan, S. & Santos-Victor, J. (2001). Real-time vision-based station keeping for underwater robots. *Proceedings of the OCEANS MTS/IEEE.*

Ziani-Cherif, S. (1998). *Contribution à la modélisation, l'estimation des paramètres dynamiques et la commande d'un engin sous-marin.* Ph. D. thesis in French, Thèse de docteur de l'Ecole Central de Nantes, France.